Estimation of the Amount of Internalized Ricin That Reaches the *trans*-Golgi Network

Bo van Deurs,* Kirsten Sandvig,‡ Ole William Petersen,* Sjur Olsnes,‡ Kai Simons,§ and Gareth Griffiths§

* Department of Anatomy, the Panum Institute, University of Copenhagen, DK-2200 Copenhagen N, Denmark; ‡ Institute for Cancer Research at the Norwegian Radium Hospital and the Norwegian Cancer Society, Oslo 3, Norway; and § European Molecular Biology Laboratory, 6900 Heidelberg, Federal Republic of Germany

Abstract. We have used a protocol for internalization of ricin, a ligand binding to plasma membrane glycoproteins and glycolipids with terminal galactosyl residues, and infection with the vesicular stomatitis virus ts 045 mutant in BHK-21 cells to determine whether internalized plasma membrane molecules tagged by ricin reach distinct compartments of the biosynthetic–exocytic pathway. At 39.5°C newly synthesized G protein of ts 045 was largely prevented from leaving the endoplasmic reticulum. At the same temperature ricin was endocytosed and reached, in addition to endosomes and lysosomes, elements of the Golgi complex. When the temperature was lowered to 19.5°C, no more ricin was delivered to the Golgi complex, but now G protein accumulated in the Golgi stacks and the *trans*-Golgi network (TGN). Double-labeling immunogold cytochemistry on ultracryosections was used to detect G protein and ricin simultaneously. These data, combined with stereological and biochemical methods, showed that ~5% of the total amount of ricin within the cells, corresponding to 6–8 × 10^4 molecules per cell, colocalized with G protein in the Golgi complex after 60 min at 39.5°C. Of this amount ~70–80% was present in the TGN. Since most of the ricin molecules remain bound to their binding sites at the low pH prevailing in compartments of the endocytic pathway, the results indicate that a fraction of the internalized plasma membrane molecules with terminal galactose are not recycled directly from endosomes or delivered to lysosomes, but are routed to the Golgi complex. Also, the results presented here, in combination with other recent studies on ricin internalization, suggest that translocation of the toxic ricin A-chain to the cytosol occurs in the TGN.

THE cell has two distinct organelle systems specialized in the sorting of membrane molecules: the Golgi complex for outward (exocytic) membrane traffic, and the endosomal system for inward (endocytic) membrane traffic (5, 9, 12, 29, 46). Considerable attention has been paid to the possible existence of a link between the exocytic and endocytic pathways, that is, whether—and to what extent—endocytosed membrane molecules are delivered to the Golgi complex (4, 5, 7, 8, 16, 17, 39, 40, 47). Two lines of argument can be advanced in support of such a connection. First, the membrane that leaves the *trans*-Golgi compartment(s) to be inserted into the plasma membrane during exocytosis must somehow be compensated for by equivalent amounts of endocytosed membrane (4, 5). Second, recent evidence indicates that a small percentage of transferrin receptors (39) as well as the mannose-6-phosphate receptors (both the 46- and 215-kD receptors; Duncan and Kornfeld, manuscript in preparation) recycle via the *trans*-Golgi compartment(s) where sialyl transferase activity is localized (6, 12, 32).

It has previously been shown that endocytosed conjugates of the toxic plant protein ricin and horseradish peroxidase (HRP)[1], as well as native ricin, detected by preembedding immunoperoxidase cytochemistry, reach a Golgi-associated compartment (10, 37, 43, 44). This compartment typically comprised an irregularly shaped, fenestrated cisternal structure with numerous branching, tubulo-vesicular profiles which were localized to one side of the Golgi stack. It thus resembled the Golgi compartment recently named the *trans*-Golgi network (TGN) (16), and previously called GERL by Novikoff (25). Since ricin binds to plasma membrane molecules with terminal galactose residues (2, 27, 34), these observations indicated that a proportion of internalized plasma membrane glycoproteins and glycolipids with terminal galactose was delivered to the TGN. Moreover, our recent data suggest that the toxic effect of ricin is coupled to the delivery to the Golgi complex (37, 44). Elegant support for this notion was recently published by Youle and Colombatti (48), who showed that a hybridoma cell secreting antibodies against ricin was resistant to the toxic effects of ricin. This observation

1. *Abbreviations used in this paper*: HRP, horseradish peroxidase; PAG, protein-A gold; TGN, *trans*-Golgi network; VSV, vesicular stomatitis virus.

is most readily explained by assuming that the internalized ricin is inactivated by the anti-ricin antibodies during their transport through the Golgi complex.

In our previous morphological studies, however, we could not conclude with certainty whether the compartment we detected with peroxidase conjugates and immunoperoxidase cytochemistry really belonged to the biosynthetic-exocytic pathway, or whether it represented a late endosomal compartment (44). In the former case we could also not decide unequivocally whether the labeled structure was on the *cis* or *trans* side of the Golgi stack. Further, we could not quantify the amount of internalized ricin that was targeted to the para-Golgi compartment by the methods used in the earlier studies.

In the present study we have used the membrane spanning protein "G" of a temperature sensitive mutant of vesicular stomatitis virus (VSV) as a marker for the Golgi stack and TGN. In the ts 045 mutant of VSV the G protein is synthesized at the nonpermissive temperature, 39.5°C, but transport out of the ER is blocked. By switching to the permissive temperature, 31°C, the G protein is transported through the Golgi complex to the plasma membrane. If, however, the temperature is changed from 39.5°C to ~20°C, the protein accumulates in high concentration in the last Golgi compartment, the TGN and, in variable amounts, in the other compartments of the Golgi stack (16). We have used a double-labeling protocol on ultracryosections with G protein as a marker for the Golgi stack/TGN in VSV-infected baby hamster kidney (BHK)-21 cells which had been simultaneously incubated with ricin. In this way we could address two important questions with respect to ricin internalization. First, is internalized ricin delivered to compartments of the Golgi complex, delineated by the G protein labeling? Second, if so, what percentage of the total internalized ricin is delivered to this (these) compartment(s)? We addressed the latter question by a combination of quantitative immunocytochemistry and biochemistry.

Materials and Methods

Cell Culture

BHK-21 cells were grown in 30- or 60-mm plastic culture dishes in the Glasgow modification of minimal essential medium (GME) with 5% FCS, 10% phosphate tryptone broth, 1 mM glutamine, penicillin, and streptomycin, 10 mM Hepes, pH 7.2. Cells were grown to confluence or near confluence (~2 d) before use.

Virus Infection and Incubation with Ricin

The cells were infected with the VSV ts 045 mutant, 40 pfu per cell. Infection was carried out for 1 h at 31°C in a high bicarbonate MEM-Hepes medium with 0.2% BSA and 1 mM glutamine. Then the medium was replaced with fresh, prewarmed medium without virus and the cells were further incubated for 3 h at 39.5°C. Subsequently, the medium was removed, a new, low bicarbonate (0.35 g/l) MEM-Hepes containing 20 μg cycloheximide per ml, preadjusted to 19.5°C, was added, and the cells incubated for 2 h at 19.5°C in a waterbath. In some experiments the cells were finally incubated for 15 min at 31°C. This incubation protocol is outlined in Fig. 1.

Ricin, at a final concentration of 10 μg/ml medium, was added to the VSV-infected cells as shown in Fig. 1. In some experiments ricin was also added to uninfected cells which were then incubated for 1 h at 37°C.

Ricin-binding Studies

The experiments were carried out in serum-free MEM-Hepes medium with

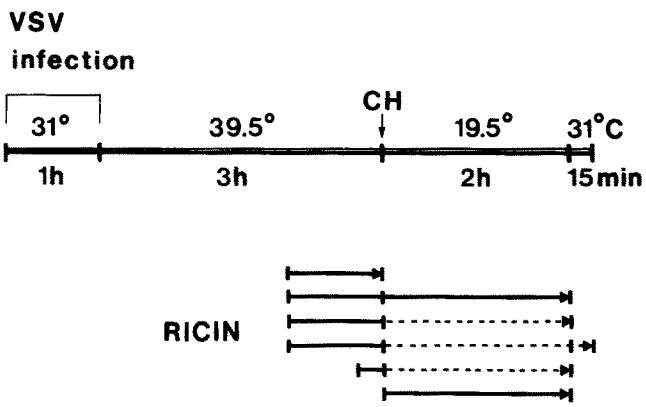

Figure 1. Schematic drawing of the experimental protocol with ricin incubation of VSV-infected cells used for the ultrastructural immunocytochemical experiments reported in this study. (⊢⊣) Incubation with 10 μg/ml ricin; (⊢- - -⊣) further incubation without ricin. The experiments were stopped by fixation as indicated (⊣). *CH*, change to fresh medium containing cycloheximide, with or without ricin. For more details, see Materials and Methods.

0.2% BSA and 2 mM glutamine. To measure binding of ricin, ^{125}I-labeled toxin was added to BHK-21 cells growing in 24-well disposable trays. After incubation for the times indicated, the cells were washed twice with PBS containing 2 mM $CaCl_2$, dissolved in 0.1 M KOH, and the cell-associated radioactivity was measured.

Endocytosed toxin was measured as the amount of lactose-resistant cell-bound toxin in the following way. After incubation with [^{125}I]ricin, the cells were incubated with PBS containing 0.1 M lactose for 5 min at 37°C and then rinsed three times in the same solution. Finally, the cell-associated radioactivity was measured.

Measurement of Protein Synthesis Inhibition

After incubation with toxin as indicated, the rate of protein synthesis was measured by incubating the cells with 1 μCi/ml [^{3}H]leucine and no unlabeled leucine for 10 min at 37°C.

The medium was then removed and the cells were treated twice with 5% wt/vol TCA. They were then dissolved in 0.1 M KOH and the radioactivity associated with the cells was measured. Control experiments showed that cells that had been exposed to monensin, ammonium chloride, or cycloheximide, and then washed, incorporated [^{3}H]leucine at essentially the same rate as untreated cells.

Immunofluorescence Studies

Cells grown on coverslips were fixed with 4% formaldehyde in PBS and permeabilized with 0.2% Triton X-100. Thereafter they were incubated with anti-ricin antibody followed by rhodamine-conjugated goat anti-rabbit antibody and finally mounted for light microscopy.

Ultrastructural Immunocytochemistry

At the end of the incubations indicated in Fig. 1, the cells were placed on ice, washed with ice-cold PBS, and fixed by adding an ice cold solution of 4% formaldehyde, 0.5% glutaraldehyde in 200 mM Pipes buffer, pH 7.2. After fixation in monolayer for ~30 min at room temperature, the cells were scraped off and centrifuged. The pellets were further fixed for ~30 min, washed with PBS, cryoprotected with 2.1 M sucrose, mounted on stubs, and frozen in liquid nitrogen. Sections were cut on an LKB CryoNova or a Sorvall MT2B ultracryomicrotome with tungsten-coated glass knives (15).

For immunocytochemistry two antibodies were used: a rabbit affinity-purified anti-G protein (luminal domain of spikes) (21), and a rabbit anti-ricin (13; a gift from Dr. D. Louvard). Incubation of sections was carried out for 30 min at room temperature. To visualize the antibodies, sections were thereafter incubated with protein A-gold (PAG) prepared according to Slot and Geuze (38) for 20 min at room temperature. Finally, the sections were contrasted with uranyl acetate and embedded in methyl cellulose (15). For single labeling experiments, 8 or 10 nm PAG was used. For double labeling,

the sections were first incubated with the anti-ricin antibody followed by 9 or 10 nm PAG, then with the anti-G protein antibody followed by 5 or 6 nm PAG (all experiments used for quantitations, and illustrated in this study). In a few experiments this pattern of labeling was reversed with respect to the gold size. Also, in a few experiments we used a monoclonal antibody to the cytoplasmic domain of the G protein (kindly provided by T. Kreis; 19) instead of the anti-G spike antibody.

The following controls were used: (*a*) incubations where the antibody was omitted; (*b*) complete incubations where protein A was used to block antibodies before incubation with PAG; and (*c*) complete incubations of cells not exposed to ricin with anti-ricin followed by PAG. (*a*) and (*b*) gave very little labeling. Thus, in (*b*) we had only 0.17 ± 0.03 (n = 11) gold particles (with 10 nm PAG) per μm^2 sectioned nucleus (see below). However, in (*c*) a higher background was found, due to unspecific binding of the anti-ricin antibody. Therefore, in complete double labeling experiments with VSV-infected cells exposed to ricin, the number of gold particles (10 nm PAG for ricin, 6 nm PAG for G protein) per μm^2 of sectioned nucleus was calculated. For anti-ricin we found 1.37 ± 0.07 (n = 22) gold particles per μm^2 of nuclear profile, and for anti-G protein 0.26 ± 0.04 (n = 10). Thus the background level produced by the anti-ricin antibody is ~8 times higher than that caused by the 10 nm PAG. The background level for G protein is so low that it can be ignored.

Quantitation

Our rationale to quantify the absolute amount of ricin in endosomes, lysosomes, and Golgi/TGN was to relate the number of gold particles to the area of organelle profile in a micrograph by point counting (see below). This area multiplied by the section thickness gives the volume of that organelle in the section. The number of gold particles over the profile is thus related to the organelle volume. Since the total volume of the endosomes, lysosomes, Golgi stack, and TGN in the BHK-21 cell was already known (Griffiths, G., R. Back, S. Swift, and M. Marsh, manuscript in preparation; Griffiths, G., S. D. Fuller, S. D. Back, S. Pfeifferank, and K. Simons, manuscript submitted for publication) we could estimate the total number of gold particles which labeled the respective organelles per cell. From this we could estimate the total number of intracellular gold particles as well as the percentage which is associated with each class of organelle per cell. Since the total amount of internalized ricin per cell could be determined biochemically, we could now relate the number of ricin molecules to the number of gold particles. In this way we could estimate the average labeling efficiency (i.e., gold per ricin) for all the intracellular organelles that contain ricin. Further, by assuming the same labeling efficiency for all the intracellular organelles we could use the number of gold particles over one class of organelle (e.g., TGN) to have an estimate of the total amount of ricin in that organelle.

It should be emphasized that for a 100% labeling efficiency there would have to be complete access of antibody to antigens and full penetration of PAG throughout the section. Any deviation from this would reduce the labeling efficiency. The access of antibody to antigens and the penetration depth of PAG remain unknown parameters. Even though there is significant penetration of label into some compartments in the section, complete accessibility of antibody and PAG is most likely only obtained for a superficial layer of the section. Nevertheless, since the labeling efficiencies that could be estimated directly in this study (the plasma membrane and the (pooled) intracellular organelles under two different experimental conditions) were all in the range of 1.8%–3.8%, we believe the above assumption is a reasonable one in the context of this study.

For the plasma membrane, whose surface area in BHK-21 cells is known (14), the number of ricin molecules bound under various conditions was determined biochemically. By division this gives the average number of bound ricin molecules per area of cell surface. This can now be related to the number of gold particles over the plasma membrane by relating the number of gold particles to intersection counts (see below), and the calculated labeling efficiency can then be compared with that obtained for the intracellular organelles.

The immunogold labeling was quantified on randomly selected cell profiles in sections with a thickness of ~0.1 μm (11, 15). To determine the amount of gold particles per μm^2 cell surface area (and per μm^2 of sectioned nucleus for background counts; see above), pictures were photographed at ×17,000 and the negatives enlarged to ×69,500 in a projector designed at EMBL. To determine the amount of gold particles per μm^3 of Golgi stacks, TGN, endosomes, and lysosome-like structures in the sections, pictures were photographed at ×28,000 and finally enlarged to ×114,500.

The quantitation was carried out largely as described by Griffiths and Hoppeler (11). The following formulae were used: (*a*) Number of gold particles per μm^2 of plasma membrane in the 0.1 μm thick sections through the cells, using a 20 mm square lattice grid is equal to $(G)/(d \times t \times I)$ where G is the number of golds, d is the distance between the lines of the lattice grid, t is the average section thickness, and I is the number of intersections.

It is important to note that this formula (*a*) is valid only when the intersections are counted in both vertical and horizontal directions. (*b*) Number of gold particles per μm^3 organelle (Golgi stack, TGN, endosome, lysosome-like structure) in the 0.1-μm thick sections through the cells, using point counting and a 10-mm square lattice grid is equal to $(G)/(P \times d^2 \times t)$ where G is the number of gold particles over the organelle profile, P is the number of points falling on the profile, d is the distance between the grid points, and t is the section thickness.

To correct the number of gold particles per organelle profile for background labeling, i.e., the number of gold particles per μm^2 sectioned (profile) nucleus (1.37/μm^2; see above), the number of gold particles per μm^2 of sectioned organelle profile (Golgi stack, TGN, endosome, lysosome, and nucleus) was first calculated using the formula (*c*): $(G)/(P \times d^2)$ and then the background value for the nucleus (1.37 golds/μm^2) was subtracted from the amount of gold per μm^2 organelle profile. The resulting value was then divided by the section thickness (t in formula *b*).

All figures in the Tables are given as mean ± SE; n = the number of pictures analyzed.

Results

Biochemical Characterization of Ricin Binding and Uptake

It is well established that ricin binds with high affinity to a variety of plasma membrane glycoproteins and glycolipids with terminal galactosyl residues (2, 27). To measure the extent of binding to BHK-21 cells, increasing amounts of [^{125}I]ricin were added to cells and the amount of cell-bound radioactivity was measured. When the data were transformed into a Scatchard plot (Fig. 2), the total number of ricin-binding sites per BHK-21 cell was found to be 1.25×10^7. This value is in good agreement with data obtained on other cell types including other strains of BHK (18, 22, 24, 34, 35).

We also measured the binding of ricin under conditions used in the experiments outlined in Fig. 1. The endocytic uptake of ricin in BHK-21 cells was slightly higher at 39.5°C than at 37°C (data not shown). The amount of cell surface bound ricin and of ricin within the cell after incubation with ricin for 60 min at 39.5°C followed by incubation for 2 h at 19.5°C with or without ricin (see Fig. 1) is shown in Table I. The fact that the amount of lactose resistant [^{125}I]ricin associated with the cells was approximately twice as high in the cells where ricin was present not only during the 1 h at 39.5°C, but also during the following 2 h at 19.5°C, indicates that a considerable amount of ricin is internalized at 19.5°C. Immunofluorescence experiments also revealed marked uptake of ricin at 19.5°C. The ligand was localized to endosomes both throughout the cytoplasm and in a distinct perinuclear position at 19.5°C (Fig. 3).

Although it has been reported that infection with wild-type VSV strongly inhibits endocytosis in BHK-21 cells, the ts 045 mutant was found to have this effect only at the permissive temperature (45). To test whether this was also the case under our experimental conditions, we compared the uptake of ricin in ts 045 infected cells and noninfected cells after incubation for 60 min at 39.5°C followed by 2 h at 19.5°C. In agreement with Wilcox et al. (45) we found that VSV ts 045 infection had no significant influence on endocytosis under these conditions (data not shown).

To eliminate the possibility that the intracellular routing of ricin observed was due to cytopathic effects of ricin, we studied the toxic effect of ricin in BHK-21 cells by measuring the

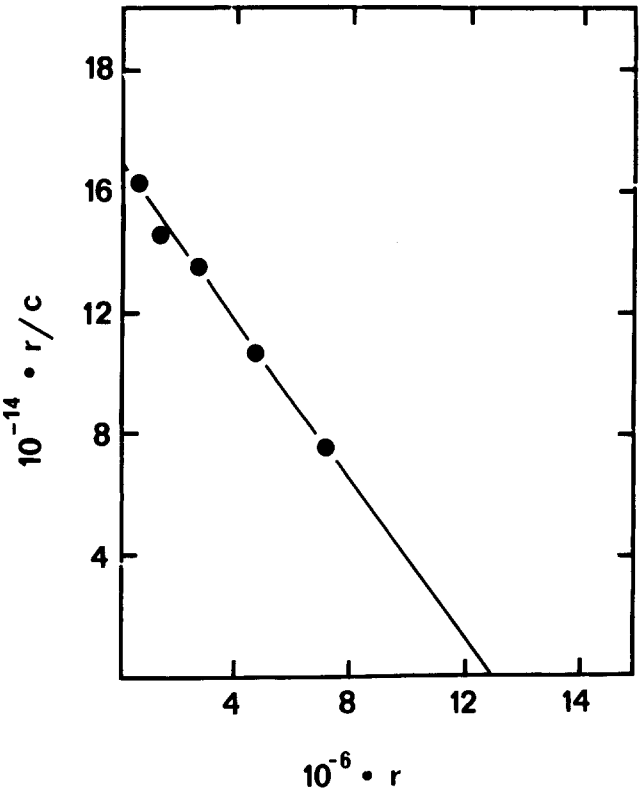

Figure 2. Scatchard plot of the binding of ^{125}I-labeled ricin to BHK-21 cells. Increasing amounts of ^{125}I-labeled ricin (127 cpm/ng) were added to cells growing in 24-well disposable trays at a density of 2.5 × 10^5 cells/well. After a 1-h incubation at 0°C, the cells were washed three times, and the cell-bound radioactivity was measured. The amount of toxin per cell was calculated and plotted according to Scatchard. (*r*) Number of toxin molecules bound per cell; (*c*) molar concentration of free toxin.

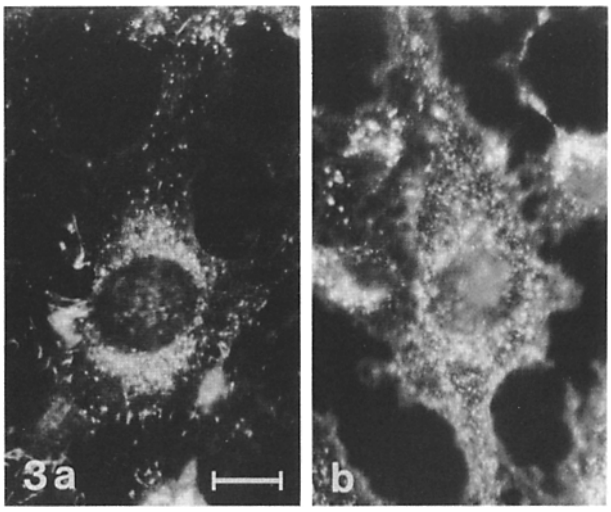

Figure 3. Immunofluorescence localization of internalized ricin (10 μg/ml) in BHK-21 cells. The cells were incubated with ricin for 1 h at 39.5°C (*a*) or for 2 h at 19.5°C (*b*) before fixation. In (*a*) the characteristic perinuclear location of ligand-containing lysosomes and endosomes is evident. (*b*) Shows that at the low temperature a marked endocytosis takes place, and that ligand-containing endosomes (which are the only labeled compartment at this temperature) are found throughout the cytoplasm as well as in a perinuclear position. Bar, 10 μm.

rate of protein synthesis after increasing periods of time. The data shown in Fig. 4 *a* demonstrate that ricin has no toxic effect after 60 min of incubation at 39.5°C. Although a pronounced inhibition in the incorporation of [^{3}H]leucine occurred between 60 and 120 min of incubation, this does not interfere with our experimental protocol (see Fig. 1). Thus, after the first 60 min of ricin incubation, the temperature was reduced to 19.5°C and, concomitantly, cycloheximide was added to prevent further protein synthesis.

As will be demonstrated below, internalized ricin is transported to the TGN. We have shown previously that compounds that induce morphological changes and interfere with functions of the Golgi complex, such as monensin, ammonium chloride, and cycloheximide, have a sensitizing effect on ricin toxicity in Vero cells and HeLa cells (33, 36, 37). The data in Fig. 4 *b* show that this is also the case in BHK-21 cells.

To use ricin as a valid label for internalized plasma membrane molecules that contain terminal galactose residues, it is necessary to establish that a significant proportion of ricin molecules remain attached to their binding sites at the low pH prevailing in compartments of the endocytic pathway (23). Control experiments with [^{125}I]ricin showed that exposure to pH 5.0 did not strongly increase the dissociation of ricin from the surface of BHK-21 cells. Thus, at pH 5.0 in the medium the amount of [^{125}I]ricin bound after 20 min

Table I. Biochemical Data on Ricin Binding and Uptake in BHK-21 Cells

Experiment	Total cell-associated ricin	Ricin on the cell surface	Ricin within the cell (lactose resistant)	Total cell-associated ricin within the cell
		× 10^6 molecules per cell		%
[^{125}I]ricin (10 μg/ml)* 60 min 39.5°C followed by 2 h 19.5°C with [^{125}I]ricin	10	8.1	1.9	19
[^{125}I]ricin (10 μg/ml) 60 min 39.5°C followed by 2 h 19.5°C without [^{125}I]ricin	3.1	2.2	0.93	30

* ^{125}I-labeled ricin: 150 cpm/ng.

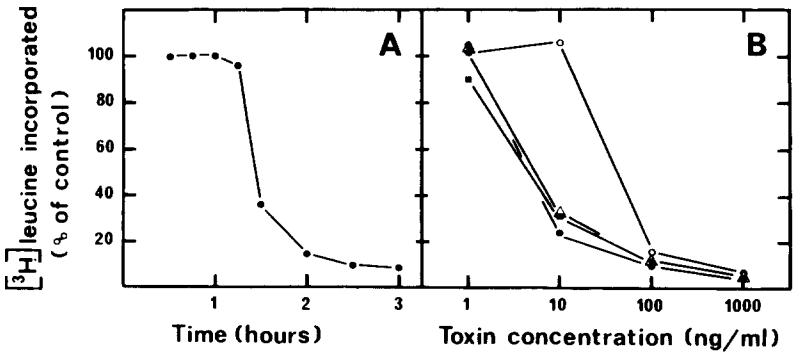

Figure 4. Effect of ricin on BHK-21 cells. (*a*) BHK-21 cells were incubated with ricin (10 μg/ml) for increasing periods of time at 39.5°C and then protein synthesis was measured as described in Materials and Methods. (*b*) BHK-21 cells were preincubated for 15 min in the absence or presence of cycloheximide, monensin, and ammonium chloride. Increasing concentrations of ricin were then added, and the incubation was continued for 3.5 h at 37°C. Finally, protein synthesis was measured during a 10-min interval as described in Materials and Methods. (●) 10^{-7} M monensin; (■) 10 μg/ml cycloheximide; (△) 10 mM NH_4Cl; (○) none.

at 37°C was 78% of the value obtained at pH 7.0 (data not shown). It should be noted that in BHK-21 cells as well as in the other cell lines (Vero, MCF-7, T47D) where we have studied the intracellular routing of ricin, an endocytic tracer that is not bound to membranes, i.e., the fluid-phase marker HRP, is not delivered to the Golgi complex (16, 20, 43, 44).

Ultrastructural Immunocytochemistry

In some experiments, uninfected BHK-21 cells were incubated with ricin for 60 min at 37°C. Ricin was then detected by immunogold labeling in endosomes and lysosomes as well as in the Golgi complex, mainly in structures which we believe represent the TGN (not shown).

BHK-21 cells were infected with VSV and incubated as outlined in Fig. 1. During the last 15 or 60 min of the 3 h period of incubation at 39.5°C, the cells were exposed to ricin. At the end of this period, G protein was localized by immunogold labeling to the ER, whereas ricin was mainly found on the cell surface, in endosomes and in lysosome-like structures. However, as expected, some ricin was also detected in Golgi-associated structures.

After further incubation at 19.5°C for 2 h, G protein was detected in Golgi stacks and the TGN (Figs. 5 and 6). Small amounts of G protein were also scattered on the cell surface (Table II), indicating that the 19.5°C temperature block for exocytosis is not completely tight. In experiments where the cells were incubated with ricin for only 15 min at 39.5°C before the 2 h at 19.5°C, ricin was confined largely to endosomes. However, after the 60 min at 39.5°C incubation with ricin before the 19.5°C incubation ricin was distinctly localized to the Golgi region (Fig. 7), and in double-labeling experiments colocalization of G protein and ricin in some Golgi cisternae and in the TGN was seen (Fig. 8). The majority of this ricin most likely reached the Golgi complex before the 19.5°C block, since we have previously shown that low temperature prevents delivery of ricin to the Golgi complex (37, 44).

In favorable sections, that is, thin sections with an optimal contrast due to uranyl acetate staining, a distinct periodicity was seen on the luminal aspect of the TGN membrane (Figs. 6 and 8 *b*) due to the dense packing of G protein (16). While the majority of the TGN profiles appeared as fenestrated sheaths and/or a system of anastomosing tubules, vacuolar portions were also encountered (Fig. 8 *c*). A pronounced variation in the degree of labeling for G protein with the anti-spike antibody was noticed. Thus, in portions of the TGN with very densely packed G protein, the corresponding gold labeling was sometimes low (Fig. 8 *b*) or even absent. This phenomenon is most likely due to steric hindrance (11). In contrast, the antibody to the cytoplasmic tail of the G protein labels most parts of the TGN extensively (not shown). With this antibody, however, the large number of G protein-associated gold particles often makes it more difficult to quantify the relatively few gold particles associated with ricin.

Quantitative data on the presence of ricin in the Golgi stacks and the TGN (as defined by colocalization with G protein in double-labeling experiments), as well as in endosomes and lysosome-like structures, are shown in Tables III and IV. It is seen that 4–6% of the total amount of ricin within the cell (depending on the experimental protocol; cf. Tables III and IV) is found together with G protein in the Golgi complex. Of this amount, at least 70–80% is present in the TGN. Relating these data to the biochemical data in Table I, we find that $\sim$6–8 × 10^4 ricin molecules are present in the Golgi complex after ricin incubation for 60 min at 39.5°C followed by 2 h at 19.5°C with or without ricin.

The total amount of gold particles in the four classes of organelles per cell after 60 min at 39.5°C followed by 2 h at 19.5°C in the presence of ricin is $\sim$3.5 × 10^4 (Table III). Comparing this amount with the number of ricin molecules within the cell as revealed by biochemical measurements ($\sim$1.9 × 10^6 molecules/cell; Table I), we obtain a labeling efficiency for the total (pooled) set of ricin-containing intracellular organelles of 1.8% (i.e., 1.8 gold particles per 100 antigens). In the same experiment we calculated a total amount of 2.6 × 10^5 gold particles associated with the cell surface per BHK-21 cell (Table V). The corresponding biochemical data showed 8.1 × 10^6 ricin molecules on the cell surface (Table I), giving a labeling efficiency of 3.2%. For the other experiment shown in Table IV a similar calculation gives labeling efficiencies of 2.7% for internal structures and 3.8% for the cell surface.

An important observation to stress here is that parts of the TGN were often found in areas of the sections without Golgi stacks in their neighbourhood (Figs. 6 and 8, *b* and *c*). This is not surprising considering the three-dimensional organization of the Golgi complex (31), but it means that many structures labeled with ricin would be difficult or impossible to classify as TGN without the use of a double-labeling protocol as in the present study. Moreover, *trans*-Golgi/TGN elements sometimes appeared dilated (Figs. 5 *c* and 8 *c*). Without a precise colocalization of G protein and ricin, many

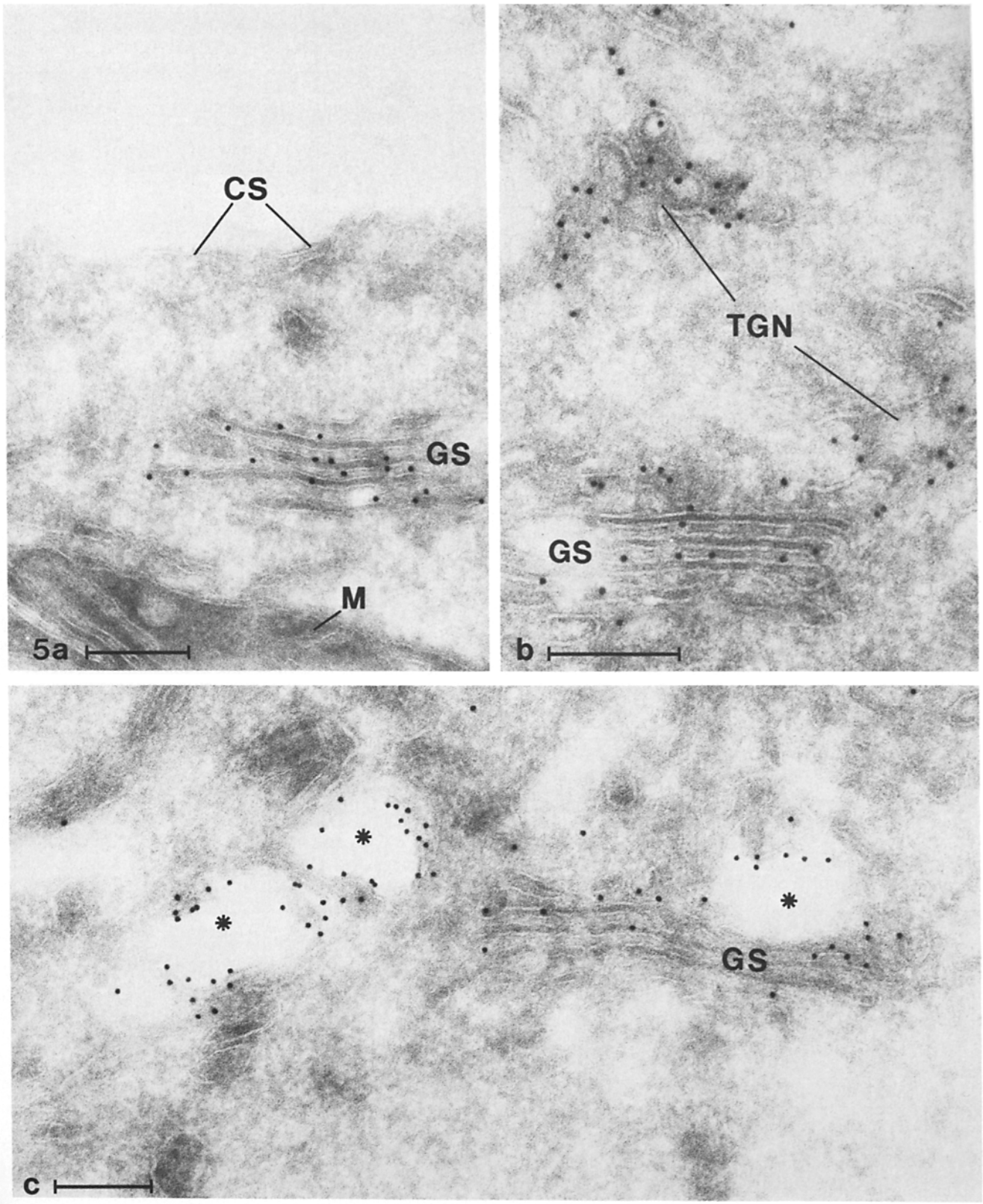

Figure 5. Appearance of the Golgi complex in BHK-21 cells infected with VSV ts 045, kept at 39.5°C for 3 h, the last 60 min with ricin, and then shifted to 19.5°C for 2 h in the presence of ricin. The cryosections have been incubated only with anti-G antibody followed by 10 nm PAG. In some parts of the sections only Golgi stacks (*GS*) are seen (*a*), while other parts show both Golgi stacks and the TGN. (*b*). Sometimes *trans*-Golgi elements/TGN are dilated or swollen (*asterisks*) (*c*). All these Golgi structures are clearly labeled for G protein. *CS*, cell surface; *M*, mitochondrion. Bars, 200 nm.

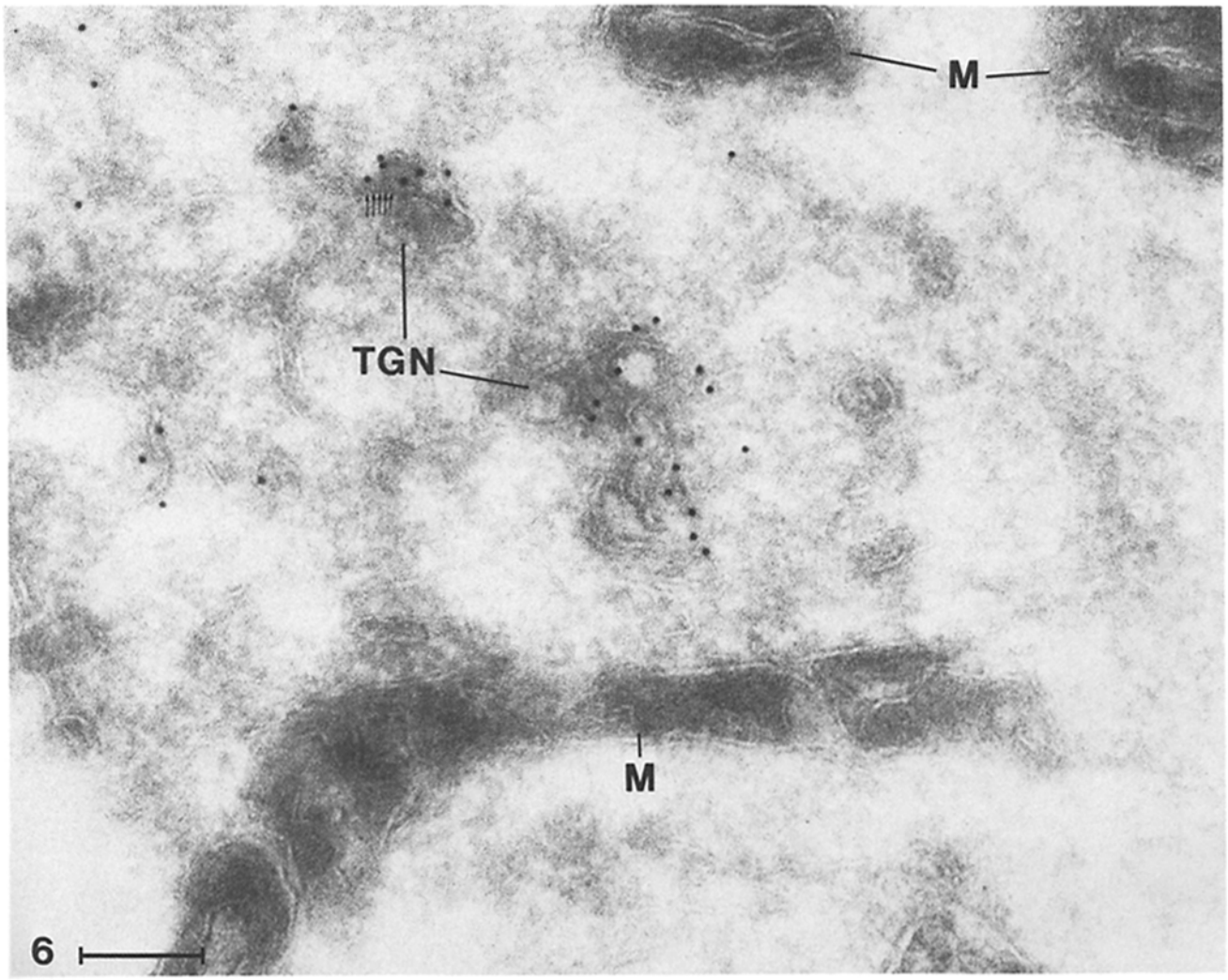

Figure 6. Appearance of the TGN in a part of a cryosection without Golgi stacks. The cells were incubated as indicated for Fig. 5, and G protein visualized with 10 nm PAG. Note the regularly spaced arrangement of G protein on the luminal aspect of the TGN membrane (*small arrows*). *M*, mitochondria. Bar, 200 nm.

such structures labeled with ricin could easily have been mistaken for endosomes.

When VSV-infected cells were exposed to ricin only at 19.5°C (for 2 h, cf. Fig. 1), label was detected over endosomes, but essentially no ricin was seen in the Golgi region. This observation confirms our previous findings of the effect of low temperature on the intracellular routing of ricin (37, 44).

Upon warming the VSV-infected, ricin-incubated cells to the permissive temperature, 31°C, for 15 min (Fig. 1), the amount of G protein in the Golgi complex had significantly decreased, and the TGN appeared more fragmented. However, distinct TGN elements with densely packed G protein, as judged by the appearance of periodically arranged structures (G protein) on the luminal side of the TGN membrane, could still be observed. These elements were labeled with ri-

Table II. Amount of G Protein on the Cell Surface of BHK-21 Cells as Detected by Immunogold Labeling (6 nm PAG)

Experiment	Gold particles/μm^2 cell surface in 0.1-μm sections	Total calculated amount of gold particles per cell surface*
VSV 3 h 39.5°C followed by 2 h 19.5°C	2.79 ± 0.43 (n = 26)	9.5×10^3
VSV 3 h 39.5°C followed by 2 h 19.5°C and then 15 min 31°C	32.90 ± 3.0 (n = 29)	1.1×10^5

* The surface area of BHK-21 cells is 3,400 μm^2 (see reference 14).

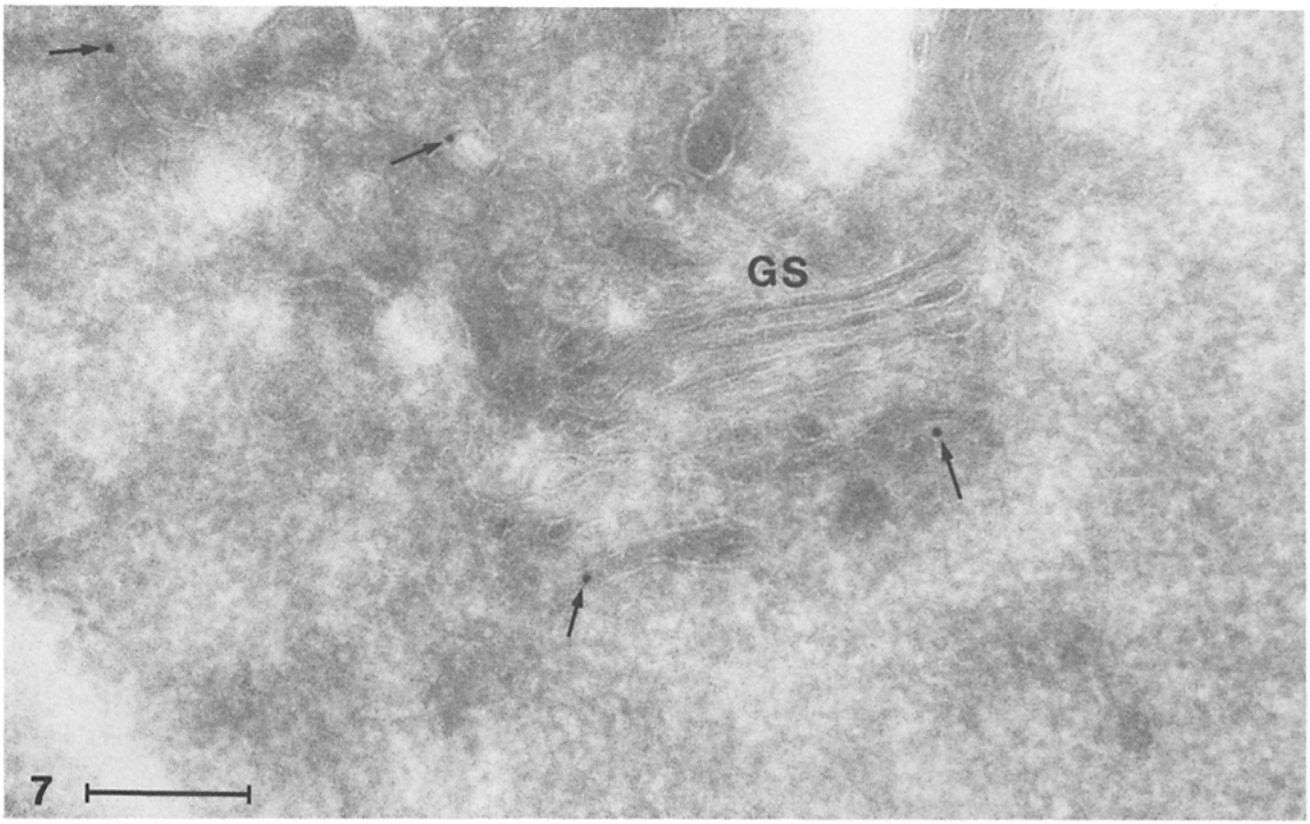

Figure 7. Cryosection of a VSV-infected cell exposed to ricin as indicated for Fig. 5. The section has only been incubated with anti-ricin followed by 10 nm PAG. Ricin is present in Golgi-associated structures (*arrows*), but it is not possible to further define the nature of the ricin-containing compartments. *GS*, Golgi stack. Bar, 200 nm.

cin (Fig. 9). Under these experimental conditions, G protein was seen in high concentrations on the cell surface (Table II), together with ricin. While the distribution of ricin on the plasma membrane was fairly uniform, G protein often occurred in high concentrations on microvilli (Fig. 10). Budding virions labeled for G protein could also be observed (Fig. 11 *b*). Moreover, G protein and ricin (and occasionally virions) now colocalized in peripheral endosomes (Fig. 11, *a*, *c*, and *d*).

Discussion

We show here that a proportion of endocytosed ricin is delivered to the Golgi complex. After 60 min of incubation with ricin, we found that 4–6% of the total amount of the internalized ricin was localized in the Golgi complex, corresponding to $\sim$6–8 $\times$ 10^4 ricin molecules. Assuming that there is only one accessible ricin-binding site per plasma membrane molecule with terminal galactose, this amount reflects the presence of 6–8 $\times$ 10^4 internalized glycoproteins and/or glycolipids in the Golgi complex. This value, which may reflect a steady state situation, is probably a slight underestimate, because some ricin molecules detach from their binding sites at the low pH in endocytic compartments.

Our observation that a small but distinct proportion of internalized plasma membrane molecules with terminal galactose is routed to the TGN is in agreement with previous studies by Snider and Rogers (39). These authors found that desialylated transferrin receptors were slowly recycled ($t_{1/2}$ = 2–3 h) and reappeared on the cell surface in a sialylated form, indicating that they must have passed through that compartment(s) of the Golgi complex where the sialyl transferase resides. Both immunocytochemical (32) and biochemical (6) data indicate that most, if not all, of this enzyme activity must reside in the TGN. We wanted to follow the routing of ricin to the Golgi complex for longer periods of time, but the marked toxicity of ricin shortly after 60 min of incubation did not allow this. At shorter incubation times, e.g., 15 min, at 39.5°C almost no ricin was present in the Golgi complex.

The present findings must also be considered with respect to vesicular traffic between the individual Golgi compart-

Figure 8. Cryosections of VSV-infected cells exposed to ricin as shown in Figs. 5–7, but here incubated first with anti-ricin followed by 10 nm PAG, and thereafter with anti-G protein followed by 6 nm PAG. The Golgi stacks (*GS*) in *a* as well as the TGN in *a–c* are labeled for G protein. Ricin, as revealed by 10 nm PAG, is indicated by arrows. Note the dilated part of the TGN (*asterisk*) in *c* containing both ricin and G protein. *CS*, cell surface; *M*, mitochondria. Bars, 200 nm.

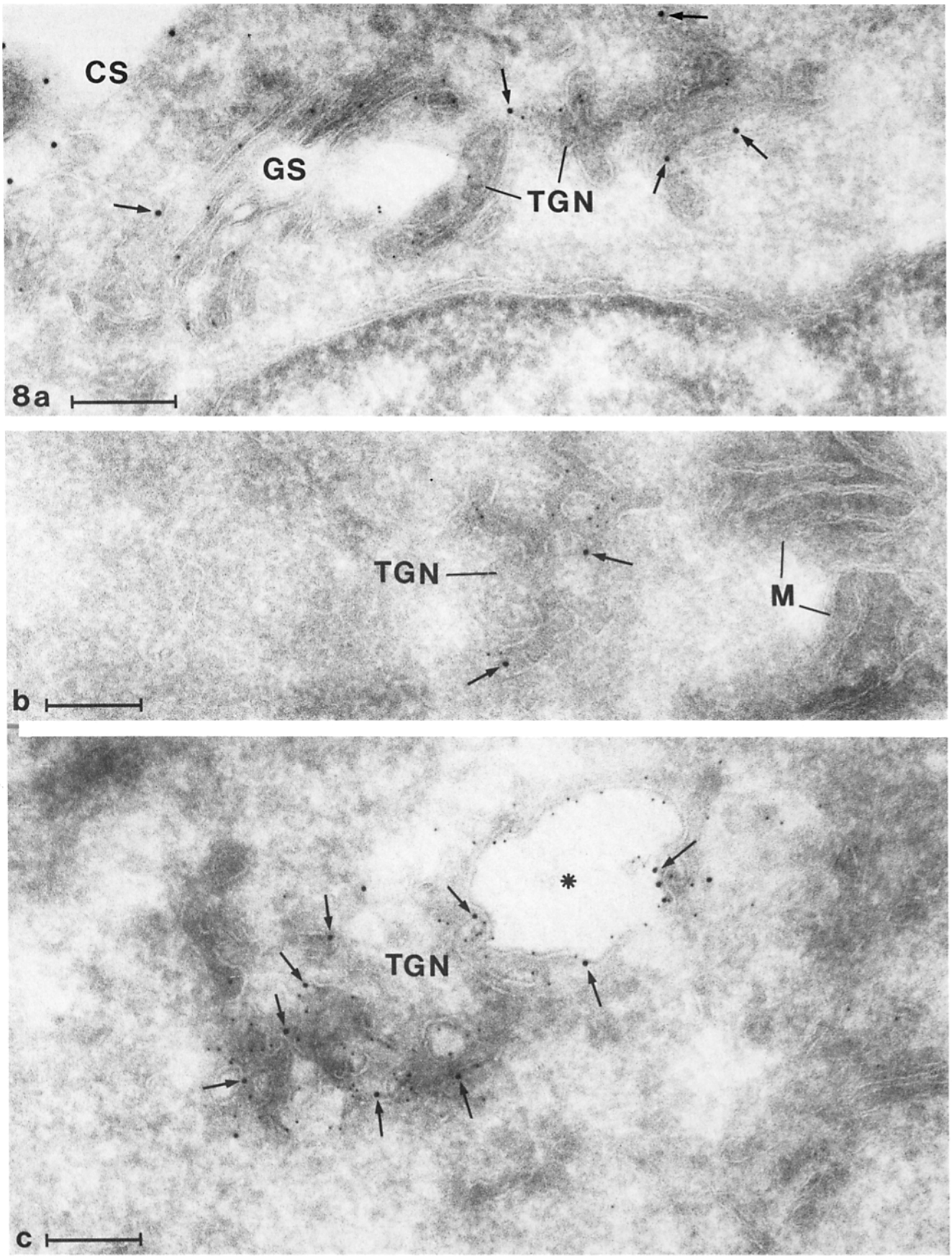
CS
GS
TGN
8a
TGN
M
b
*
TGN
c

*Table III. Amount of Ricin in Intracellular Compartments of BHK-21 Cells as Detected by Immunogold Labeling (10 nm PAG). * Ricin Incubation for 60 min at 39.5°C Followed by 2 h at 19.5°C with Ricin*

Compartment	Gold particles/μm^3 compartment in 0.1-μm thick sections of the cells‡	Total volume of the compartment per cell§	Calculated amounts of gold particles per compartment per cell
		μm^3	
Golgi stacks‖	32.1 ± 8.3 (n = 40)	12.78	410
TGN‖	102.9 ± 11.9 (n = 57)	9.83	1,012
Endosomes	1108.4 ± 119.3 (n = 28)	19.9	22,057
Lysosome-like structures	160.4 ± 57.4 (n = 16)	71.8	11,517
Total ~3.5×10^4			

* For details, see Materials and Methods.
‡ All values have been corrected for background labeling.
§ Data from Griffiths et al. (manuscript submitted for publication, and manuscript in preparation).
‖ Ricin-gold labeling of Golgi stacks and TGN was established by colocalization with gold labeling (6 nm PAG) for G protein.

Table IV. Ricin Incubation for 60 min at 39.5°C Followed by 2 h at 19.5°C Without Ricin

Compartment	Gold particles/μm^3 compartment in 0.1-μm thick sections of the cells*	Total volume of the compartment per cell‡	Calculated amounts of gold particles per compartment per cell
		μm^3	
Golgi stacks§	24.3 ± 6.2 (n = 18)	12.78	311
TGN§	124.7 ± 10.1 (n = 24)	9.83	1,226
Endosomes	733.2 ± 82.0 (n = 26)	19.9	14,591
Lysosome-like structures	124.5 ± 33.7 (n = 18)	71.8	8,939
Total ~2.5×10^4			

* All values have been corrected for background labeling.
‡ Data from Griffiths, G., R. Back, S. Swift, and M. Marsh, manuscript in preparation; Griffiths, G., S. D. Fuller, S. D. Back, S. Pfeifferank, and K. Simons, manuscript submitted for publication.
§ Ricin-gold labeling of Golgi stacks and TGN was established by colocalization with gold labeling (6 nm PAG) for G protein.

Table V. Amount of Ricin on the Cell Surface of BHK-21 Cells as Detected by Immunogold Labeling (10 nm PAG)

Experiment	Gold particles/μm^2 cell surface in 0.1-μm sections	Total calculated amount of gold particles per cell surface*
30 min at 4°C with ricin	86.3 ± 11.3 (n = 33)	2.9×10^5
60 min at 39.5°C with ricin followed by 2 h at 19.5°C with ricin	76.2 ± 5.4 (n = 28)	2.6×10^5
60 min at 39.5°C with ricin followed by 2 h at 19.5°C without ricin	24.3 ± 1.2 (n = 24)	8.3×10^4

* The surface area of BHK-21 cells is 3,400 μm^2 (see reference 14).

ments (*cis*-, medial-, and *trans*) as well as between the TGN and the plasma membrane. Since the size of the Golgi compartments normally stays constant, it is clear that for every vesicle that leaves a certain compartment there must be an equivalent amount of membrane that recycles back. Consider, for example, the traffic between the TGN and the plasma membrane. The vesicles that transport G protein from the TGN to the plasma membrane have been visualized in the living cell (1) and, less conclusively, at the ultrastructural level in VSV-infected cells after releasing the 20°C block, a condition where large amounts of the G protein are transported from the TGN to the cell surface (16). In contrast, attempts to follow the pathway from the plasma membrane to the TGN, a traffic which may either be direct or occur via endosomes (4), have been far less conclusive, although both non-specific and specific markers for plasma membrane molecules have been unambiguously shown to reach the stacked Golgi cisternae (4, 5, 47). We are convinced that the delivery of ricin to the Golgi complex/TGN in the cell types we have studied occurs via endosomes, for two reasons (44). First, time sequence studies have consistently revealed ricin in endosomes before it is detected in Golgi elements. Second, a direct pathway from the plasma membrane to the Golgi complex would necessitate a sorting step at the plasma membrane to separate the Golgi pathway from the endosome pathway. The fact that a number of studies have shown that different cell surface receptors are internalized in the same coated pits argues against such a sorting

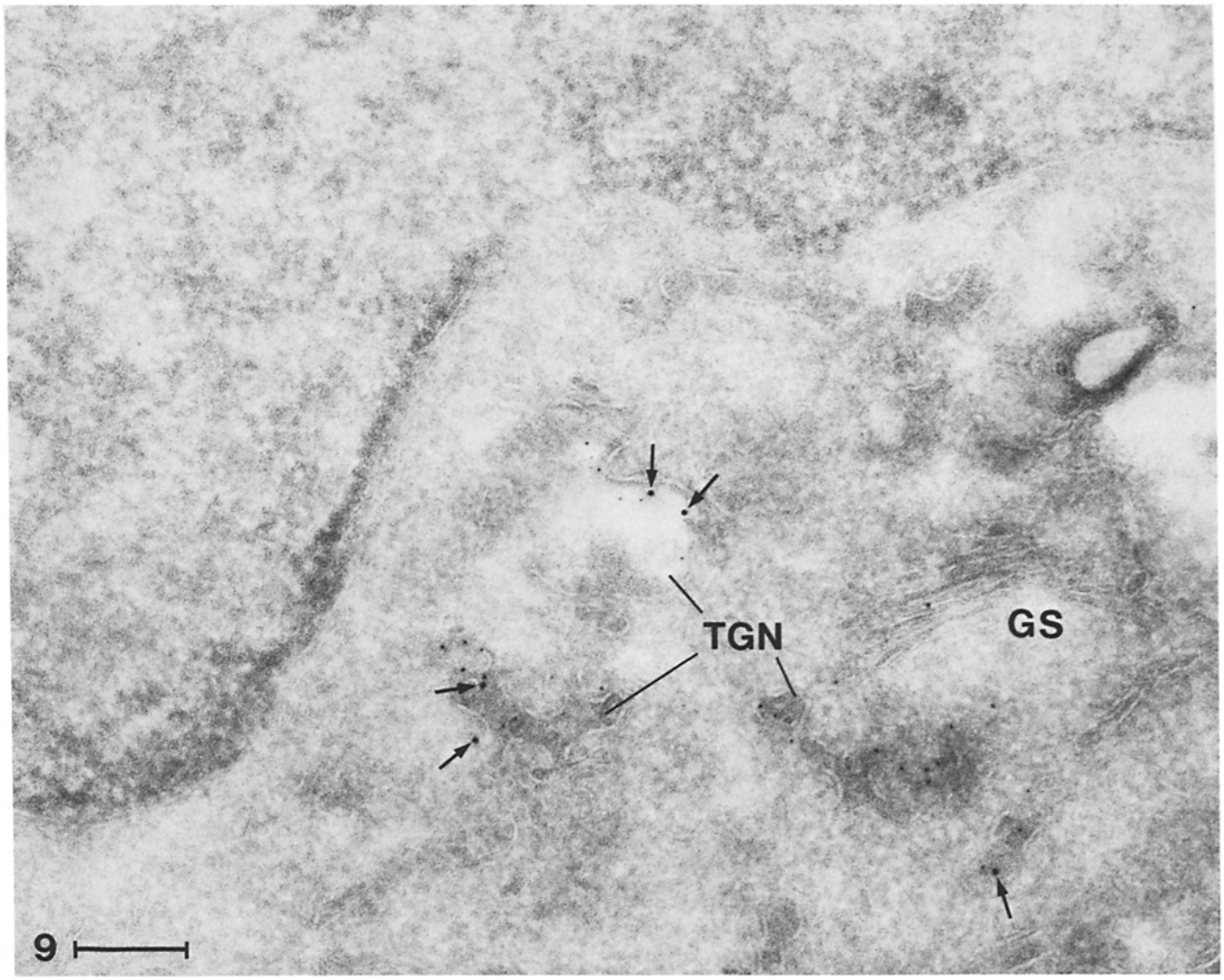

Figure 9. Appearance of the Golgi complex of VSV-infected cells incubated with ricin for 1 h at 39.5°C, then for 2 h at 19.5°C without ricin, and finally for 15 min at 31°C. The Golgi stack (*GS*) and in particular the TGN still shows G protein as detected by 6 nm PAG. Moreover, the TGN is labeled for ricin by 10 nm PAG (*arrows*). Bar, 200 nm.

(9). We have shown previously that both native ricin and various mono- and polyvalent ricin conjugates are taken up and rapidly reach endosomes. Here sorting takes place, since only native ricin and monovalent conjugates are routed to the Golgi complex (42–44). There are only few qualitative (3, 4, 28), and no quantitative, studies that have unequivocally shown that a marker for a cell surface protein or lipid can be delivered to bona fide (exocytic) Golgi compartments. The large number of studies that claim to have shown this are hampered by the difficulty that, in the absence of double labeling experiments, it may be difficult, if not impossible, to unequivocally distinguish the TGN from endosome compartments (12).

Our observation that ricin is present in both the Golgi stack and the TGN, although most frequent in the latter compartment (ratio ~1:4), may be explained in two ways: (*a*) all ricin in the Golgi complex has been delivered exclusively to the TGN from where some molecules are sent back to the preceding stacked cisternae, and (*b*) ricin, or rather, the plasma membrane molecules to which ricin is bound, are also delivered directly to Golgi cisternae. At present we cannot determine which explanation is the correct one. An added complication here is that the TGN consists of both a cisternal and a tubulo-reticular part. The cisternal part represents roughly 10% of the total surface area of this compartment in BHK-21 cells infected with VSV at 20°C (Griffiths, G., R. Back, S. Swift, and M. Marsh, manuscript in preparation). This cisternal part of the TGN is morphologically indistinguishable from the cisternae that comprise the preceding Golgi compartments. This makes it difficult to say precisely how much of the gold label observed over the Golgi stack is attributable to the TGN. We can, however, conclude that at least 70–80% of the Golgi associated ricin is in the TGN.

Using morphological approaches to define the Golgi compartment(s) where exocytic and endocytic membrane traffic possibly meet, two serious problems should be considered. First, as shown here and elsewhere (16, 31), the TGN may extend far away from the Golgi stacks and thus may be found in random sections without any apparent contiguity to Golgi stacks. Accordingly, the TGN can be detected unequivocally

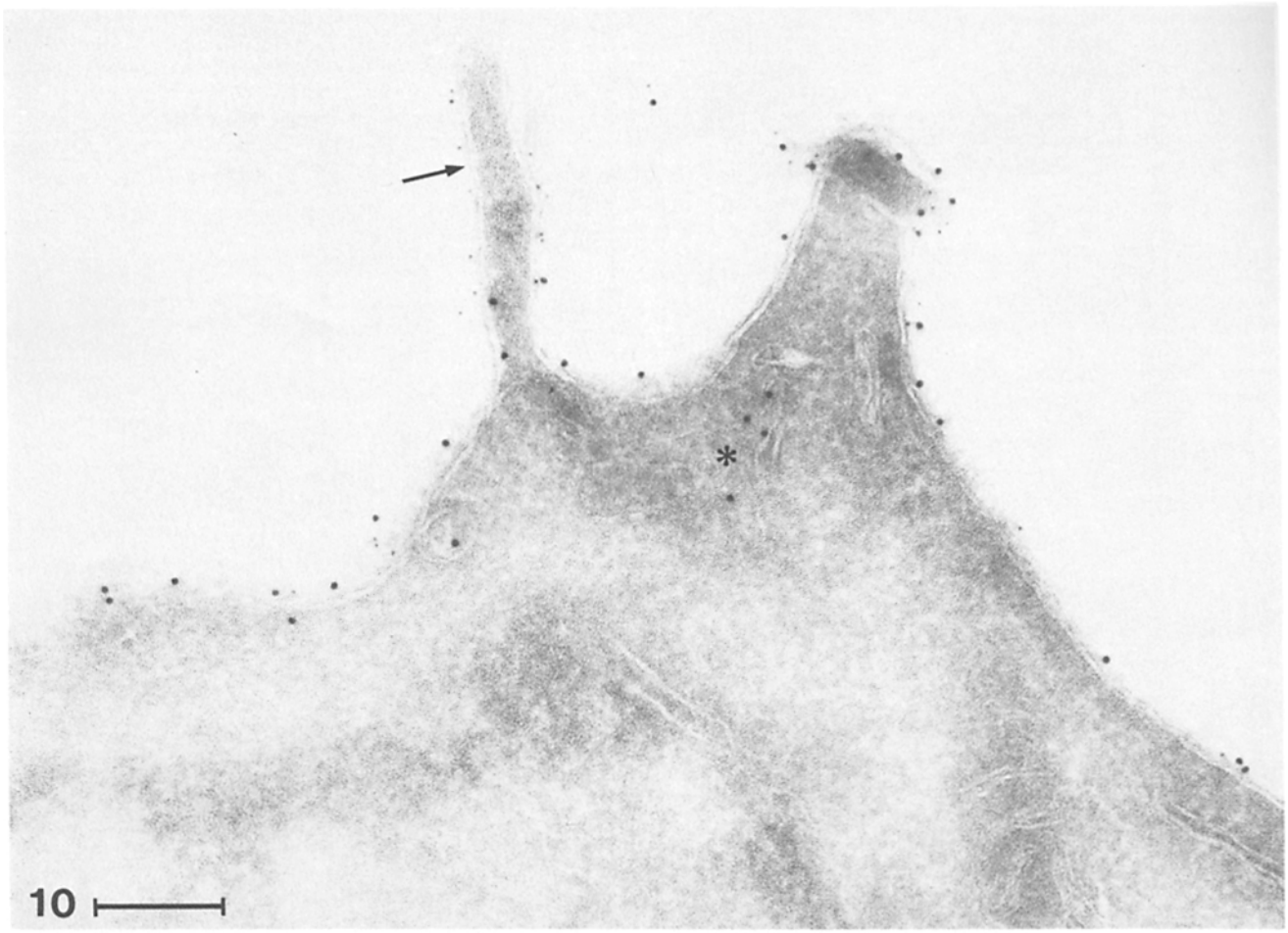

Figure 10. Part of the surface of a BHK-21 cell incubated as indicated in Fig. 9. Both ricin (10 nm PAG) and G protein (6 nm PAG) are seen on the cell surface. Labeling for G protein is most prominent on a microvillus (*arrow*). The asterisk indicates ricin–gold labeling of a presumptive peripheral endosome. Bar, 200 nm.

only by using specific markers of the biosynthetic-exocytic pathway such as VSV G protein, to distinguish it from elements of the endosomal system. Moreover, it is also well established that the endosomal system is highly pleomorphic (20, 42, 44) and that endosomal elements may be present close to the Golgi complex or even be intercalated with Golgi elements. A good example of these problems is illustrated in a recent paper by Orci et al. (26) where structures containing internalized HRP were found in various positions within the Golgi stack. Again, the application of specific markers is required to distinguish between endosomal elements and the Golgi complex (here defined strictly as a series of compartments on the biosynthetic-exocytic pathway).

The second problem to be considered is that to obtain a rough estimate of the proportion of internalized molecules being delivered to the Golgi complex, particulate markers such as colloidal gold have to be used. Although peroxidase is a useful gross marker of intracellular compartments (20, 43, 44) above a certain threshold concentration for the enzyme, the reaction product will be expected to fill up a given compartment completely. It must be emphasized that not only can the reaction product of HRP not be quantified, the technique can be quantitatively misleading. The high sensitivity of the method means that a quantitatively minor fraction of HRP in one structure can give a reaction product which is indistinguishable from that found in another structure with 10 or 100-fold more enzyme. In the present study, for example, using immunogold labeling we found roughly 20-fold more ricin in endosomes/lysosomes than in the Golgi/TGN. In our previous studies, however, the amount of reaction product for ricin conjugated to HRP appeared largely to be the same in these compartments (43, 44). On the other hand, ligands which are directly conjugated to particulate markers for endocytic studies may lead to an incorrect picture of the intracellular routing and distribution of the ligand. For instance, we have shown that ricin-gold, in contrast to ricin-HRP, is not transported from endosomes to the Golgi complex (43, 44). For the reasons given here it must be apparent that for future studies where the precise pathway of a ligand is to be followed quantitatively, this goal can only be reached by using double-label immunocytochemistry with particulate markers and a postembedding incubation technique. Our present results strongly support previous work which has indicated that reliable estimation of the amount of protein in a certain compartment is possible by using immunogold labeling on ultracryosections (11, 30).

The small but distinct fraction of internalized ricin that is delivered to the Golgi complex may be of crucial importance

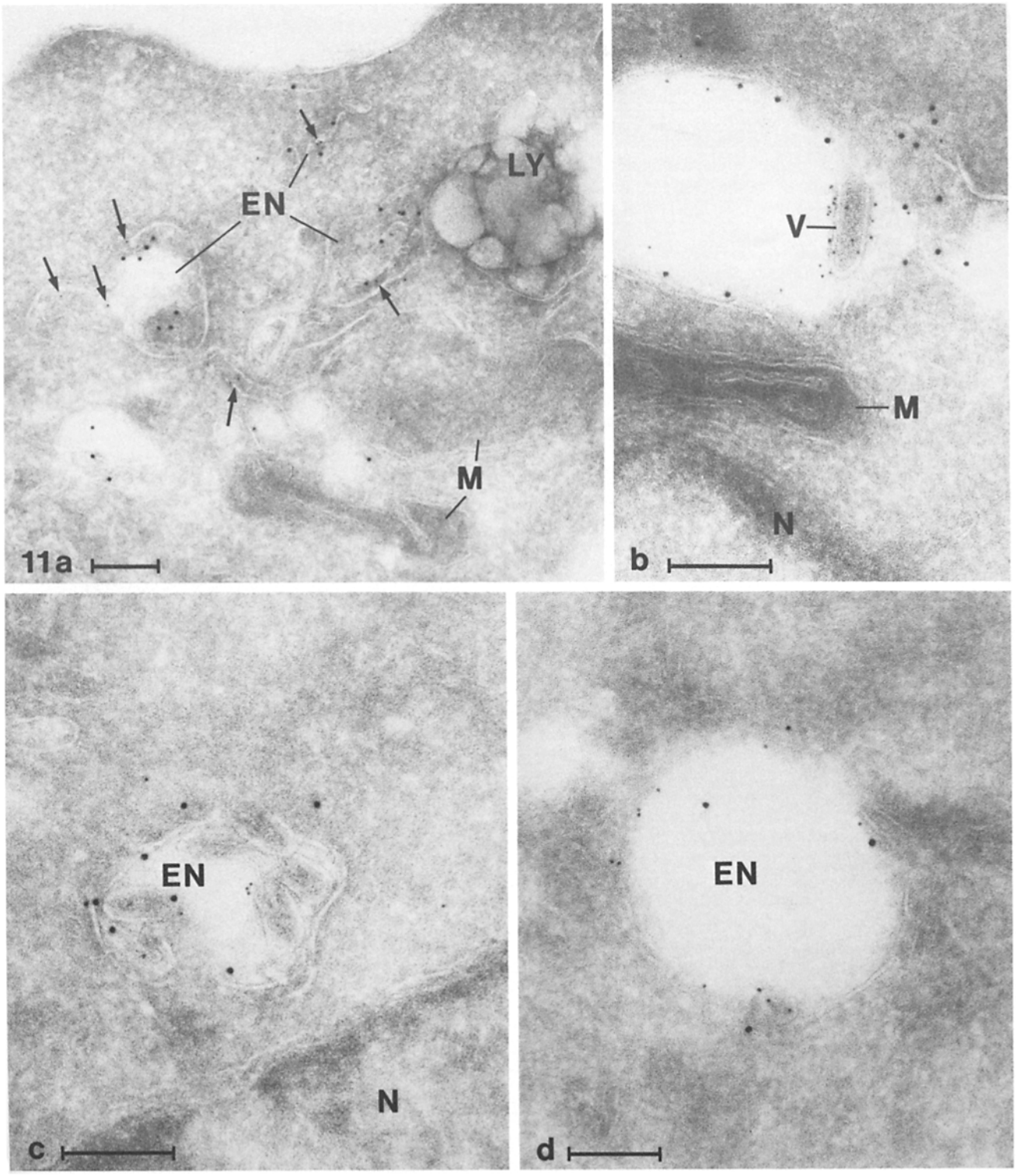

Figure 11. Parts of BHK-21 cells incubated as shown in Figs. 9 and 10. (*a*) The peripheral cytoplasm of a cell with endosomes (*EN*) labeled both for ricin (10 nm PAG) and G protein (6 nm PAG; *arrows*). The lysosome-like structure (*LY*) is unlabeled. (*b*) shows a budding VSV virion (*V*) distinctly labeled for G protein (6 nm PAG). On the adjacent cell surfaces, both G protein and ricin (10 nm PAG) are seen. *c* and *d* are endosomes (*EN*) labeled for both ricin (10 nm PAG) and G protein (6 nm PAG). In addition, the endosome in *c* contains several endocytosed virions. *M*, mitochondria; *N*, nucleus. Bars, 200 nm.

for the translocation of the ricin A-chain into the cytosol and the subsequent inhibition of the protein synthesis. Thus, the low concentrations of monensin that sensitize cells to ricin do not increase the pH in endosomes, but are known to affect the Golgi apparatus (41). The finding that the transfer of ricin to the Golgi complex as well as the toxic effect of ricin are

strongly inhibited at temperatures below 20°C (37, 44) agrees with the hypothesis that transfer to the Golgi complex is necessary for entry of ricin into the cytosol. Recently Youle and Colombatti (48) found that a hybridoma cell producing monoclonal antibodies against ricin was resistant to ricin. This indicates that the endocytosed ricin A-chain is not translocated into the cytosol before the internalized ricin molecules meet the newly synthetized anti-ricin antibodies, and that this meeting takes place in the Golgi complex, most likely the TGN.

We thank Ruth Back, Michael Hollinshead, Jorunn Jacobsen, Keld Ottosen, and Hilkka Virta for excellent technical assistance, and Dr. Ivan de Curtis for his help in providing cultures of BHK-21 cells.

We also thank Dr. E. I. Christensen, Dr. R. C. Hallowes, and Dr. J. Gruenberg for their critical reading of the manuscript, and Drs. J. Duncan and S. Kornfeld for providing us with an unpublished manuscript on the mannose-6-phosphate receptor.

The anti-ricin antibody and the anti-G tail monoclonal antibody were a kind gift of Drs. Daniel Louvard and Thomas Kreis, respectively.

B. van Deurs was supported by a European Molecular Biology Organization (EMBO) short term fellowship during most of this work, and by the NOVO Foundation and the Danish Medical Research Council. Kirsten Sandvig and Sjur Olsnes were supported by the Norwegian Cancer Society.

Received for publication 6 August 1987, and in revised form 21 October 1987.

References

1. Arnheiter, H., M. Dubois-Dalcq, and R. A. Lazzarini. 1984. Direct visualization of protein transport and processing in the living cell by microinjection of specific antibodies. *Cell.* 39:99-109.
2. Baenziger, J. U., and D. Fiete. 1979. Structural determinants of ricinus communis agglutinin and toxin specificity for oligosaccharides. *J. Biol. Chem.* 254:9795-9799.
3. Balin, B. J., and R. D. Broadwell. 1987. Lectin-labeled membrane is transferred to the Golgi complex in mouse pituitary cells in vivo. *J. Histochem. Cytochem.* 35:489-498.
4. Farquhar, M. G. 1978. Recovery of surface membrane in anterior pituitary cells. Variations in traffic detected with anionic and cationic ferritin. *J. Cell Biol.* 77:R35-R42.
5. Farquhar, M. G. 1985. Progress in unraveling pathways of Golgi traffic. *Annu. Rev. Cell Biol.* 1:447-488.
6. Fuller, S. D., R. Bravo, and K. Simons. 1985. An enzymatic assay reveals that proteins destined for the apical or basolateral domains of an epithelial cell line share the same late Golgi compartments. *EMBO (Eur. Mol. Biol. Org.) J.* 4:297-307.
7. Geuze, H. J., J. W. Slot, G. J. E. M. Strous, H. F. Lodish, and A. L. Schwartz. 1983. Intracellular site of asialoglycoprotein receptor-ligand uncoupling: Double-label immunoelectron microscopy during receptor-mediated endocytosis. *Cell.* 32:277-287.
8. Geuze, H. J., J. W. Slot, J. P. Luzio, and A. L. Schwartz. 1984. A cycloheximide-resistant pool of receptors for asialoglycoproteins and mannose 6-phosphate residues in the Golgi complex of hepatocytes. *EMBO (Eur. Mol. Biol. Org.) J.* 3:2677-2685.
9. Goldstein, J. L., M. S. Brown, R. G. W. Anderson, D. W. Russell, and W. J. Schneider. 1985. Receptor-mediated endocytosis: concepts emerging from the LDL receptor system. *Annu. Rev. Cell Biol.* 1:1-39.
10. Gonatas, N. K., S. U. Kim, A. Stieber, and S. Avrameas. 1977. Internalization of lectins in neuronal GERL. *J. Cell Biol.* 73:1-13.
11. Griffiths, G., and H. Hoppeler. 1986. Quantitation in immunocytochemistry: correlation of immunogold labeling to absolute number of membrane antigens. *J. Histochem. Cytochem.* 34:1389-1398.
12. Griffiths, G., and K. Simons. 1986. The trans Golgi network: sorting at the exit site of the Golgi complex. *Science (Wash. DC).* 234:438-443.
13. Griffiths, G., R. Brands, B. Burke, D. Louvard, and G. Warren. 1982. Viral membrane proteins acquire galactose in trans Golgi cisternae during intracellular transport. *J. Cell Biol.* 95:781-792.
14. Griffiths, G., G. Warren, P. Quinn, O. Mathieu-Costello, and H. Hoppeler. 1984. Density of newly synthesized plasma membrane proteins in intracellular membranes. I. Stereological studies. *J. Cell Biol.* 98:2133-2141.
15. Griffiths, G., A. McDowall, R. Back, and J. Dubochet. 1984. On the preparation of cryosections for immunocytochemistry. *J. Ultrastruct. Res.* 89:65-78.
16. Griffiths, G., S. Pfeiffer, K. Simons, and K. Matlin. 1985. Exit of newly synthesized membrane proteins from trans cisterna of the Golgi complex to the plasma membrane. *J. Cell Biol.* 101:949-964.
17. Hedman, K., K. L. Goldenthal, A. V. Rutherford, I. Pastan, and M. C. Willingham. 1987. Comparison of the intracellular pathways of transferrin recycling and vesicular stomatitis virus membrane glycoprotein exocytosis by ultrastructural double-label cytochemistry. *J. Histochem. Cytochem.* 35:233-243.
18. Hyman, R., M. Lacorbiere, S. Stavarek, and G. Nicolson. 1974. Derivation of lymphoma variants with reduced sensitivity to plant lectins. *J. Natl. Cancer Inst.* 52:963-969.
19. Kreis, T. E. 1986. Microinjected antibodies against the cytoplasmic domain of vesicular stomatitis virus glycoprotein block its transport to the cell surface. *EMBO (Eur. Mol. Biol. Org.) J.* 5:931-941.
20. Marsh, M., G. Griffiths, G. E. Dean, I. Mellman, and A. Helenius. 1986. Three-dimensional structure of endosomes in BHK-21 cells. *Proc. Natl. Acad. Sci. USA.* 83:2899-2903.
21. Matlin, K. S., H. Reggio, A. Helenius, and K. Simons. 1982. Pathway of vesicular stomatitis virus entry leading to infection. *J. Mol. Biol.* 156: 609-631.
22. Meager, A., A. Ungkitchanukit, and R. C. Hughes. 1976. Variants of hamster fibroblasts resistant to ricinus communis toxin (ricin). *Biochem. J.* 154:113-124.
23. Mellman, I., R. Fuchs, and A. Helenius. 1986. Acidification of the endocytic and exocytic pathways. *Annu. Rev. Biochem.* 55:663-700.
24. Nicolson, G., M. Lacorbiere, and W. Eckhart. 1975. Qualitative and quantitative interactions of lectins with untreated and neuraminidase-treated normal, wild-type and temperature-sensitive polyoma-transformed fibroblasts. *Biochemistry.* 14:172-179.
25. Novikoff, A. B. 1976. The endoplasmic reticulum: A cytochemist's view (a review). *Proc. Natl. Acad. Sci. USA.* 73:2781-2787.
26. Orci, L., M. Ravazzola, M. Amherdt, D. Brown, and A. Perrelet. 1986. Transport of horseradish peroxidase from the cell surface to the Golgi in insulin-secreting cells: preferential labeling of cisternae located in an intermediate position in the stack. *EMBO (Eur. Mol. Biol. Org.) J.* 5:2097-2101.
27. Pardoe, G. I., G. W. G. Bird, and G. Uhlenbruck. 1969. On the specificity of lectins with a broad agglutination spectrum. The nature of the specific receptors of Ricinus communis and Solanum tuberosum lectins. *Z. Immunitatsforsch.* 137:442-457.
28. Patzak, A., and H. Winkler. 1986. Exocytic exposure and recycling of membrane antigens of chromaffin granules: ultrastructural evaluation after immunolabeling. *J. Cell Biol.* 102:510-515.
29. Pfeffer, S. R., and J. E. Rothman. 1987. Biosynthetic protein transport and sorting by the endoplasmic reticulum and Golgi. *Annu. Rev. Biochem.* 56:829-852.
30. Posthuma, G., J. W. Slot, and H. J. Geuze. 1987. Usefulness of the immunogold technique in quantitation of a soluble protein in ultra-thin sections. *J. Histochem. Cytochem.* 35:405-410.
31. Rambourg, A., Y. Clermont, and L. Hermo. 1981. Three-dimensional structure of the Golgi apparatus. *Methods Cell Biol.* 23:155-166.
32. Roth, J., D. J. Taatjes, J. M. Lucocq, J. Weinstein, and J. C. Paulson. 1985. Demonstration of an extensive trans-tubular network continuous with the Golgi apparatus stack that may function in glycosylation. *Cell.* 43:287-295.
33. Sandvig, K., and S. Olsnes. 1982. Entry of the toxic proteins abrin, modeccin, ricin, and diphtheria toxin into cells. II. Effect of pH, metabolic inhibitors, and ionophores and evidence for toxin penetration from endocytic vesicles. *J. Biol. Chem.* 257:7504-7513.
34. Sandvig, K., S. Olsnes, and A. Pihl. 1976. Kinetics of binding of the toxic lectins abrin and ricin to surface receptors of human cells. *J. Biol. Chem.* 251:3977-3984.
35. Sandvig, K., S. Olsnes, and A. Pihl. 1978. Binding, uptake and degradation of the proteins abrin and ricin by toxin-resistant cell variants. *Eur. J. Biochem.* 82:13-23.
36. Sandvig, K., S. Olsnes, and A. Pihl. 1979. Inhibitory effect of ammonium chloride and chloroquine on the entry of the toxic lectin modeccin into HeLa cells. *Biochem. Biophys. Res. Commun.* 90:648-655.
37. Sandvig, K., T. I. Tønnessen, and S. Olsnes. 1986. Ability of inhibitors of glycosylation and protein synthesis to sensitize cells to abrin, ricin, shigella toxin, and pseudomonas toxin. *Cancer Res.* 46:6418-6422.
38. Slot, J. W., and H. J. Geuze. 1985. A new method of preparing gold probes for multiple-labeling cytochemistry. *Eur. J. Cell Biol.* 38:87-93.
39. Snider, M. D., and O. C. Rogers. 1985. Intracellular movement of cell surface receptors after endocytosis: resialylation of asialo-transferrin receptor in human erythroleukemia cells. *J. Cell Biol.* 100:826-834.
40. Snider, M. D., and O. C. Rogers. 1986. Membrane traffic in animal cells: cellular glycoproteins return to the site of Golgi mannosidase I. *J. Cell Biol.* 103:265-275.
41. Tartakoff, A. M. 1983. Perturbation of vesicular traffic with the carboxylic ionophore monensin. *Cell.* 32:1026-1028.
42. van Deurs, B., L. Ryde Pedersen, A. Sundan, S. Olsnes, and K. Sandvig. 1985. Receptor-mediated endocytosis of a ricin-colloidal gold conjugate in Vero cells. Intracellular routing to vacuolar and tubulo-vesicular portions of the endosomal system. *Exp. Cell Res.* 159:287-304.
43. van Deurs, B., T. I. Tønnessen, O. W. Petersen, K. Sandvig, and

S. Olsnes. 1986. Routing of internalized ricin and ricin conjugates to the Golgi complex. *J. Cell Biol.* 102:37–47.
44. van Deurs, B., O. W. Petersen, S. Olsnes, and K. Sandvig. 1987. Delivery of internalized ricin from endosomes to cisternal Golgi elements is a discontinuous, temperature-sensitive process. *Exp. Cell Res.* 171:137–152.
45. Wilcox, D. K., P. A. Whitaker-Dowling, J. S. Youngner, and C. C. Widnell. 1983. Rapid inhibition of pinocytosis in baby hamster kidney (BHK-21) cells following infection with vesicular stomatitis virus. *J. Cell Biol.* 97:1444–1451.
46. Wileman, T., C. Harding, and P. Stahl. 1985. Receptor-mediated endocytosis. *Biochem. J.* 232:1–14.
47. Woods, J. W., M. Doriaux, and M. G. Farquhar. 1986. Transferrin receptors recycle to cis and middle as well as trans Golgi cisternae in Ig-secreting myeloma cells. *J. Cell Biol.* 103:277–286.
48. Youle, R. J., and M. Colombatti. 1987. Hybridoma cells containing intracellular anti-ricin antibodies show ricin meets secretory antibody before entering the cytosol. *J. Biol. Chem.* 262:4676–4682.